

## Direct amine-functionalisation of $\gamma$ -Fe<sub>2</sub>O<sub>3</sub> nanoparticles

Cite this: *Dalton Trans.*, 2014, **43**, 2948

V. Rocher,<sup>a</sup> J. Manerova,<sup>b</sup> M. Kinnear,<sup>a</sup> D. J. Evans<sup>a</sup> and M. G. Francesconi<sup>\*a</sup>

Received 29th August 2013,  
Accepted 25th November 2013

DOI: 10.1039/c3dt52386a

www.rsc.org/dalton

A novel and simple preparation of amine-modified  $\gamma$ -Fe<sub>2</sub>O<sub>3</sub> nanoparticles is described. The presence of amine groups on the surface, instead of hydroxyl groups, will allow conjugation of biologically active molecules to the iron oxide nanoparticles without the need for a size increasing silica shell. Furthermore, the outer amine-layer increases the temperature of the  $\gamma$ -Fe<sub>2</sub>O<sub>3</sub> to  $\alpha$ -Fe<sub>2</sub>O<sub>3</sub> structural transition in a similar way to previously reported cationic substitutions. This may suggest the formation of an oxide-nitride outer layer. Re-dispersion of the amine-modified  $\gamma$ -Fe<sub>2</sub>O<sub>3</sub> nanoparticles led to the preparation of stable ferrofluids.

## Introduction

A simple route was used to prepare a ferrofluid from nanoparticles directly functionalised with amine groups. Ferrofluids are generally made of nanoparticles of iron oxide dispersed into a liquid medium to form a stable colloidal solution.<sup>1</sup> The magnetic moment carried by the nanoparticles makes these dispersions responsive to external magnetic fields<sup>2</sup> opening up a number of interesting potential applications.<sup>3–5</sup> In order to obtain stable ferrofluids, aggregation between the magnetic nanoparticles must be avoided and, generally, this is achieved by functionalisation, *e.g.* surface binding of molecules to create steric hindrance,<sup>6</sup> either directly on the nanoparticles' surface or through additional silica shells. By careful choice of the molecule, the properties of ferrofluids can be tailored towards different applications. Direct functionalisation can be achieved by bonding molecules to hydroxyl groups present on the surface of the nanoparticles, the advantage being that the size of the nanoparticles is maintained as there is no need for an additional silica shell. The requirement for amine-functionalised nanoparticles is dictated by certain types of molecules, for example complex biologically active molecules, which will bind to the nanoparticles *via* an amide bond.<sup>7</sup>

Ferrofluids are most commonly dispersions of either  $\gamma$ -Fe<sub>2</sub>O<sub>3</sub> (maghemite) or Fe<sub>3</sub>O<sub>4</sub> (magnetite) nanoparticles or a mixture of both. The two structures of  $\gamma$ -Fe<sub>2</sub>O<sub>3</sub> and Fe<sub>3</sub>O<sub>4</sub> are

both based on a FCC lattice of O<sup>2–</sup> anions, with Fe<sub>3</sub>O<sub>4</sub> containing both Fe<sup>2+</sup> and Fe<sup>3+</sup> cations, and  $\gamma$ -Fe<sub>2</sub>O<sub>3</sub> Fe<sup>3+</sup> cations and cation vacancies to maintain charge neutrality.<sup>8–10</sup> Under thermal treatment cubic, ferromagnetic maghemite transforms irreversibly into the rhombohedral antiferromagnetic hematite ( $\alpha$ -Fe<sub>2</sub>O<sub>3</sub>).<sup>11</sup> This structural transition is being investigated with the aim of increasing the temperature limit of stability of the maghemite phase to maintain its magnetic properties and widen the applicability of  $\gamma$ -Fe<sub>2</sub>O<sub>3</sub>. For example,  $\gamma$ -Fe<sub>2</sub>O<sub>3</sub> shows high sensitivity and selectivity in sensors for hydrocarbon gases, without the need for a noble metal.<sup>12</sup> Cation doping of  $\gamma$ -Fe<sub>2</sub>O<sub>3</sub> nanoparticles seems to be the most effective way to increase the temperature of the  $\gamma$ -Fe<sub>2</sub>O<sub>3</sub>/ $\alpha$ -Fe<sub>2</sub>O<sub>3</sub> transition, but very little has been reported on transition temperature variations caused by functionalisation. Here we report that reacting  $\gamma$ -Fe<sub>2</sub>O<sub>3</sub> nanoparticles with NH<sub>3</sub> (g) at 200 °C for 2–4 hours leads to direct functionalisation of the nanoparticles with amine groups and increases the temperature of the structural transition from  $\gamma$ -Fe<sub>2</sub>O<sub>3</sub> (maghemite) to  $\alpha$ -Fe<sub>2</sub>O<sub>3</sub> (hematite) up to 550 °C. This suggests the possibility of formation of an outer layer of iron oxide-nitride.

## Experimental

### Preparation of nanoparticles of $\gamma$ -Fe<sub>2</sub>O<sub>3</sub>

Iron oxide nanoparticles were prepared *via* a sol-gel process.<sup>13</sup> A solution of iron(II) and iron(III) chlorides in water was reacted with ammonium hydroxide to form magnetite (Fe<sub>3</sub>O<sub>4</sub>) nanoparticles. After washing with acetone and ether, the nanoparticles were re-dispersed in nitric acid. Reaction with iron(III) nitrate at boiling point oxidised the nanoparticles to maghemite ( $\gamma$ -Fe<sub>2</sub>O<sub>3</sub>).

<sup>a</sup>Department of Chemistry, University of Hull, Cottingham Road, Hull, HU6 7RX, UK.  
E-mail: m.g.francesconi@hull.ac.uk; Fax: +44 (0)1482 46 6410;  
Tel: +44 (0)1482 46 5409

<sup>b</sup>Chemical and Biological Engineering Department, The University of Sheffield, Sir Robert Hadfield Building, Mappin Street, Sheffield, S1 3JD, UK.  
E-mail: j.manerova@sheffield.ac.uk; Fax: +44 (0)114 222 7501;  
Tel: +44 (0)114 222 7500



### Amination of $\gamma\text{-Fe}_2\text{O}_3$ nanoparticles with $\text{NH}_3$ (g)

Dried nanoparticles of  $\gamma\text{-Fe}_2\text{O}_3$  were placed into a small ceramic reaction boat, which was placed at the centre of the tube in a tube furnace. The flow rate of ammonia gas was  $4.0 \text{ L h}^{-1}$  and excess was removed by an HCl scrubber. The temperature was raised to  $200^\circ\text{C}$  at  $5^\circ\text{C min}^{-1}$  and maintained between 1 and 2 hours. At the end of the reaction, the tube was flushed with nitrogen to remove unreacted ammonia and the product was transferred to a glove box for storage under argon.

Ferrofluids were prepared by dispersion of  $\gamma\text{-Fe}_2\text{O}_3$  nanoparticles and amine-modified  $\gamma\text{-Fe}_2\text{O}_3$  nanoparticles. A sample of approximately 100 mg was added to 2 mL of aqueous solution of  $\text{HNO}_3$  ( $\text{pH} = 2$ ). This suspension was then subjected to 30 minutes of ultrasonic radiation to break the larger aggregates. The resulting colloidal dispersions were left to rest for 24 hours to test their stability.

Powder X-ray diffraction was carried out using a Siemens D5000 diffractometer using the  $\text{Cu K}\alpha$  radiation. Data were recorded from  $2\theta = 10^\circ$  to  $2\theta = 110^\circ$  over 72 hours, with a step size of  $0.02^\circ$ .

Thermogravimetric analyses were carried out using a Mettler TGA/DSC 1 Starsystem. 10–15 mg of nanoparticles were placed in an alumina pan and heated at a constant rate ( $30^\circ\text{C min}^{-1}$ ) to  $900^\circ\text{C}$  under air, with the weight pattern and heat flow recorded as functions of the temperature.

The nitrogen content of the N-doped samples was measured using a CE Instruments 1108 CHN analyzer and results were expressed as weight percentages.

Nitrogen adsorption isotherms were recorded on a Micromeritics Tristar 3000. Size distribution was calculated from these data using the BJH model.

To demonstrate qualitatively the presence of surface amine groups, portions of ferrofluids formed with  $\gamma\text{-Fe}_2\text{O}_3$  nanoparticles and  $\gamma\text{-Fe}_2\text{O}_3$  nanoparticles reacted with ammonia were reacted for 1 h with a solution of fluorescamine (4'-phenylspiro[2-benzofuran-3,2'-furan]-1,3'-dione) in acetone (1 mg in 5 mL). The nanoparticles were then removed by filtration and the presence of fluorophors was revealed by examining the solutions under UV light.

Mössbauer spectra were recorded in zero magnetic field at 80 K on an ES-Technology MS-105 Mössbauer spectrometer with a  $900 \text{ MBq } ^{57}\text{Co}$  source in a rhodium matrix at ambient temperature. Spectra were referenced against a  $25 \mu\text{m}$  iron foil at 298 K and spectrum parameters were obtained by fitting with Lorentzian curves. Samples were ground with boron nitride before mounting in the sample holder.

## Results and discussion

The size of the nanoparticles, calculated from nitrogen adsorption data, shows sizes distributed between 4.5 nm and 6.0 nm for initial  $\gamma\text{-Fe}_2\text{O}_3$  particles and between 5.5 nm and 7.0 nm for  $\gamma\text{-Fe}_2\text{O}_3$  reacted with ammonia; the reaction with ammonia caused only a limited increase of the size of the  $\gamma\text{-Fe}_2\text{O}_3$

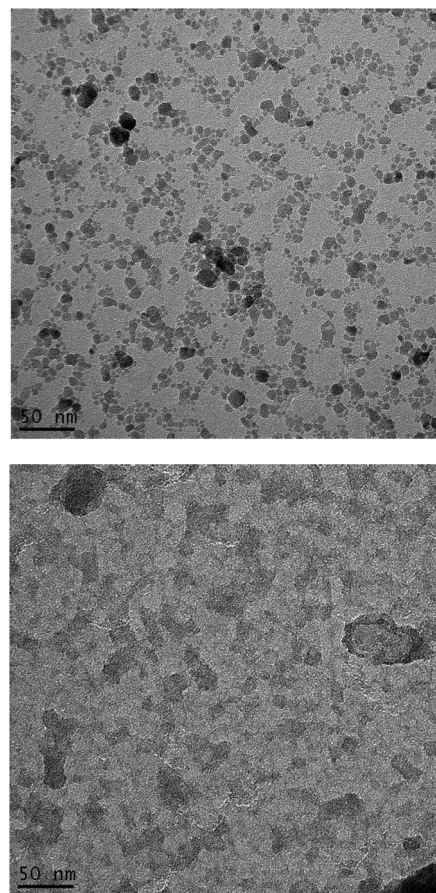


**Fig. 1** TEM images of  $\gamma\text{-Fe}_2\text{O}_3$  nanoparticles (top) and  $\gamma\text{-Fe}_2\text{O}_3$  nanoparticles reacted with ammonia at  $200^\circ\text{C}$  for 2 hours (bottom).

nanoparticles, although aggregation took place after reaction with ammonia gas, as shown by TEM images (Fig. 1).

Stable colloidal suspensions (ferrofluids) were obtained by sonication in de-ionised water using both  $\gamma\text{-Fe}_2\text{O}_3$  nanoparticles and  $\gamma\text{-Fe}_2\text{O}_3$  nanoparticles reacted with ammonia.

Powder X-ray diffraction (PXRD) of  $\gamma\text{-Fe}_2\text{O}_3$  nanoparticles and  $\gamma\text{-Fe}_2\text{O}_3$  nanoparticles reacted with  $\text{NH}_3$  (g) for 1 and 2 hours at  $200^\circ\text{C}$  are shown in Fig. 2. The PXRD pattern of the  $\gamma\text{-Fe}_2\text{O}_3$  nanoparticles shows the  $\gamma\text{-Fe}_2\text{O}_3$  single phase. The percentage of  $\gamma\text{-Fe}_2\text{O}_3$  versus  $\text{Fe}_3\text{O}_4$  was calculated *via* a peak deconvolution method to be 98.66%.<sup>14</sup> The  $\gamma\text{-Fe}_2\text{O}_3$  structure is maintained after ammoniation at  $200^\circ\text{C}$  up to 2 hours and no formation of impurities can be detected. The unit cell parameters of all three compounds were refined from the general model for spinel-type structures, *i.e.* a face-centred cubic unit cell (space group  $Fd\bar{3}m$ , number 227). No substantial difference was observed between the unit cell parameters of the three samples analysed ( $a = 8.349(1) \text{ \AA}$  for  $\gamma\text{-Fe}_2\text{O}_3$ ;  $a = 8.337(2) \text{ \AA}$  for  $\gamma\text{-Fe}_2\text{O}_3 + \text{NH}_3$  (g) for 1 hour;  $a = 8.335(1) \text{ \AA}$  for  $\gamma\text{-Fe}_2\text{O}_3 + \text{NH}_3$  (g) for 2 hours).<sup>17,18</sup> The findings of the refinements are in agreement with those reported by Petkov *et al.*<sup>19</sup> The nitrogen content (weight%) was determined by elemental analysis to be 0.05% and 0.24% for nanoparticles reacted with ammonia for 1 and 2 hours, respectively.



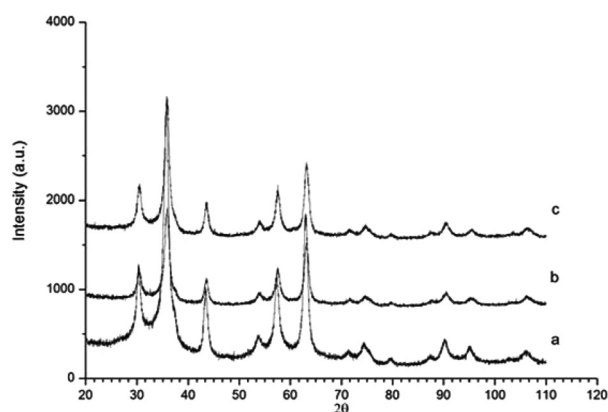


Fig. 2 PXRD diffractograms of  $\gamma$ -Fe<sub>2</sub>O<sub>3</sub> nanoparticles before and after reaction with NH<sub>3</sub> for different times. (a) Initial  $\gamma$ -Fe<sub>2</sub>O<sub>3</sub> nanoparticles; (b) nanoparticles reacted for 1 hour; (c) nanoparticles reacted for 2 hours.

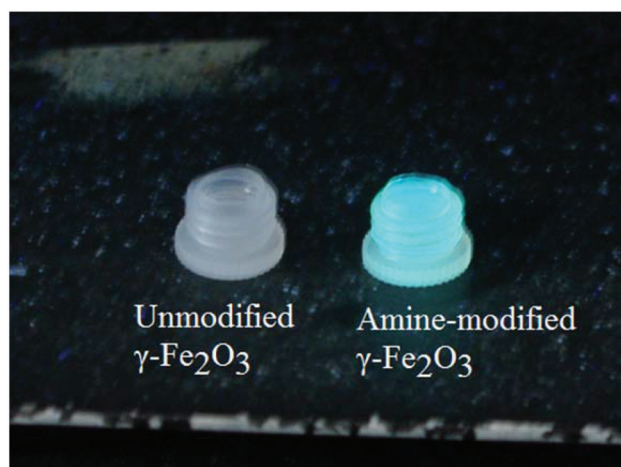


Fig. 3 Fluorescamine test showing fluorescence only on reaction with amine-modified  $\gamma$ -Fe<sub>2</sub>O<sub>3</sub> nanoparticles.

Reactions of both  $\gamma$ -Fe<sub>2</sub>O<sub>3</sub> nanoparticles and ammoniated  $\gamma$ -Fe<sub>2</sub>O<sub>3</sub> nanoparticles with fluorescamine were carried out to investigate qualitatively the presence of amine groups on the surface of the ammoniated  $\gamma$ -Fe<sub>2</sub>O<sub>3</sub> nanoparticles.<sup>15</sup> Fluorescamine does not fluoresce itself but, after reaction with amine functional groups, forms a highly fluorescent fluorophor. Furthermore, fluorescamine is specific for primary amines as it does not react with secondary amines and forms a non-fluorescent adduct with ammonia.<sup>16</sup> The formation of fluorophors was observed only for the nanoparticles that had been reacted with ammonia (Fig. 3), indicating that primary amines have replaced a portion of the hydroxide groups on the surface of the  $\gamma$ -Fe<sub>2</sub>O<sub>3</sub> nanoparticles. Further evidence of amine-functionalisation is the pH of the ferrofluid suspensions, which was consistently between 11 and 12.

Reactions between Fe<sub>3</sub>O<sub>4</sub>,  $\alpha$ -Fe<sub>2</sub>O<sub>3</sub> and Fe with NH<sub>3</sub> and/or NH<sub>3</sub>/H<sub>2</sub> at temperatures between 350 and 900 °C have resulted in a variety of iron nitrides.<sup>20–23</sup> Tessier *et al.* and Kikkawa

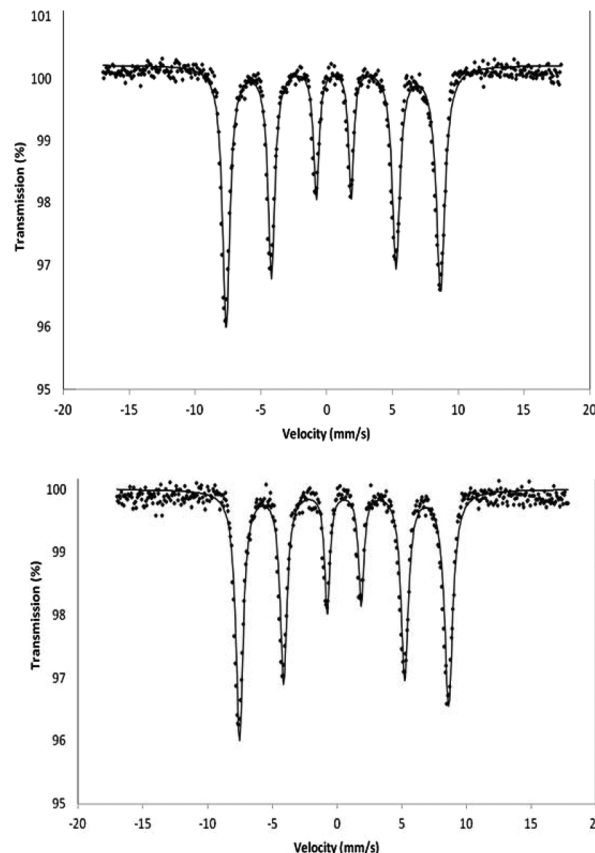


Fig. 4 Mössbauer spectrum of  $\gamma$ -Fe<sub>2</sub>O<sub>3</sub> (top) and  $\gamma$ -Fe<sub>2</sub>O<sub>3</sub> after 2 hours treatment with ammonia (bottom) recorded in the solid state at 80 K in zero magnetic field.

*et al.* reported the formation of Fe<sub>16</sub>N<sub>2</sub> via a 'soft chemistry' route, *i.e.* by using low temperatures and long times, reacting  $\alpha$ -Fe<sub>2</sub>O<sub>3</sub> with ammonia for 10 days at 110 °C<sup>24</sup> or for 100 hours at 130 °C, after reduction of  $\alpha$ -Fe<sub>2</sub>O<sub>3</sub> to  $\alpha$ -Fe.<sup>25</sup> In our work, low temperature and short reaction times have led to breakage of bonds between the surface of the nanoparticles and –OH groups and to their replacement with –NH<sub>2</sub> groups, as well as the probable formation of a thin oxide–nitride layer. The fact that PXRD showed no structural changes and/or secondary phases, the small nitrogen content detected *via* elemental analyses, and the results from the fluorescamine experiment eliminate the formation of an iron nitride and support direct functionalisation of  $\gamma$ -Fe<sub>2</sub>O<sub>3</sub> nanoparticles with amine groups.

Zero-field Mössbauer spectra for  $\gamma$ -Fe<sub>2</sub>O<sub>3</sub> and  $\gamma$ -Fe<sub>2</sub>O<sub>3</sub> nanoparticles after ammoniation were recorded (Fig. 4). The spectrum for each sample is indistinguishable from the other and confirms that the  $\gamma$ -Fe<sub>2</sub>O<sub>3</sub> structure is maintained on ammoniation. There is no evidence for magnetite or significant amounts of impurity being present. Only one hyperfine pattern is observed as expected in zero field and the spectra correspond to those previously reported for  $\gamma$ -Fe<sub>2</sub>O<sub>3</sub>.<sup>26,27</sup>

The TGA and heat flow diagram for  $\gamma$ -Fe<sub>2</sub>O<sub>3</sub> nanoparticles heated in air (Fig. 5, top) shows an initial sharp weight loss due to physisorbed and chemisorbed moisture and hydroxyl





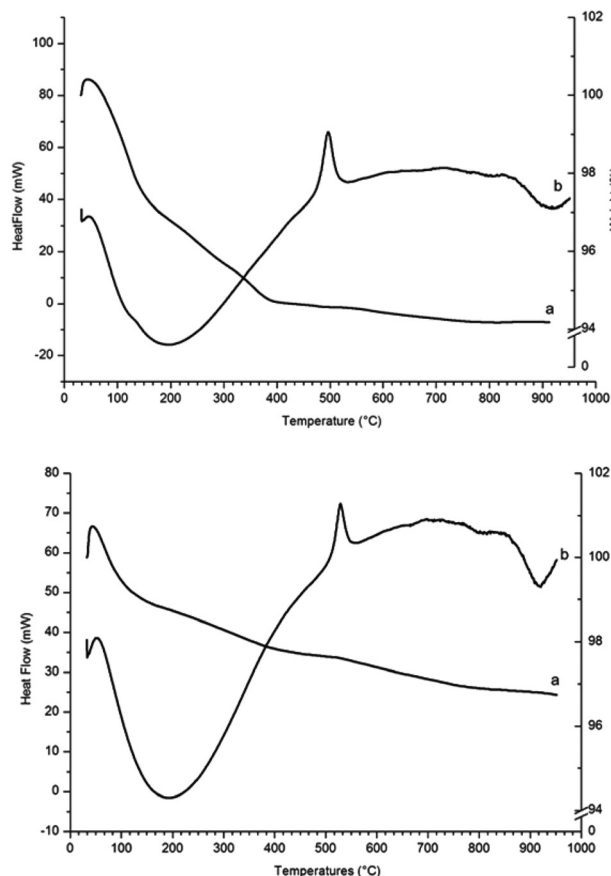


Fig. 5 TGA and DSC analysis in air of  $\gamma$ -Fe<sub>2</sub>O<sub>3</sub> nanoparticles (top) and  $\gamma$ -Fe<sub>2</sub>O<sub>3</sub> nanoparticles reacted with NH<sub>3</sub> (g) for 2 hours at 200 °C (bottom) ((a) weight of the sample as percentage of initial weight; (b) heat flow).

groups. The heat flow shows a large exothermic peak at 495 °C corresponding to transformation of  $\gamma$ -Fe<sub>2</sub>O<sub>3</sub> into  $\alpha$ -Fe<sub>2</sub>O<sub>3</sub>, in agreement with the transition temperature reported by E. Darezereshki, who focussed on  $\gamma$ -Fe<sub>2</sub>O<sub>3</sub> nanoparticles of similar size (13 and 19 nm).<sup>28</sup> The residue samples from TGA analyses were analysed by PXRD and the patterns showed only diffraction peaks belonging to the  $\alpha$ -Fe<sub>2</sub>O<sub>3</sub> phase.

The TGA and heat flow diagrams for  $\gamma$ -Fe<sub>2</sub>O<sub>3</sub> nanoparticles reacted with NH<sub>3</sub> (g) for 2 hours at 200 °C (Fig. 5, bottom) show a weight loss between room temperature and 400 °C that is probably due to loss of amino groups from the surface of the nanoparticles. The heat flow shows that the exothermic peak corresponding to transformation of  $\gamma$ -Fe<sub>2</sub>O<sub>3</sub> into  $\alpha$ -Fe<sub>2</sub>O<sub>3</sub> has shifted from 495 °C to 550 °C.

A comparison of the exothermic heat flow peaks indicating the  $\gamma$ -Fe<sub>2</sub>O<sub>3</sub> to  $\alpha$ -Fe<sub>2</sub>O<sub>3</sub> transition temperature, for all three samples, is shown in Fig. 6. The transition temperature increases from 495 °C for the  $\gamma$ -Fe<sub>2</sub>O<sub>3</sub> nanoparticles to 526 °C for  $\gamma$ -Fe<sub>2</sub>O<sub>3</sub> nanoparticles reacted with NH<sub>3</sub> (g) for 1 hour, and to 550 °C for the  $\gamma$ -Fe<sub>2</sub>O<sub>3</sub> nanoparticles reacted with NH<sub>3</sub> (g) for 2 hours.

The maghemite–hematite structural transition has been discussed in a recent review on polymorphous transformation

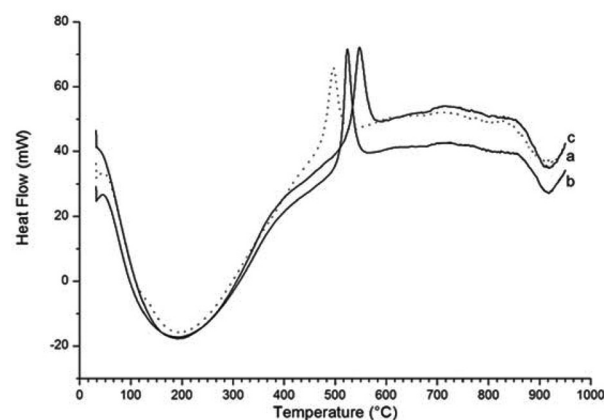


Fig. 6 Comparison of the heat flow diagrams for (a)  $\gamma$ -Fe<sub>2</sub>O<sub>3</sub> nanoparticles (dotted line) and (b)  $\gamma$ -Fe<sub>2</sub>O<sub>3</sub> nanoparticles reacted for 1 hour and (c) for 2 hours.

of nanometric iron(III) oxides.<sup>29</sup> The maghemite to hematite phase transition was studied using differential thermal analysis<sup>30</sup> and *in situ* real time X-ray diffraction.<sup>31,32</sup> Different transition temperatures have been reported for nanoparticles of maghemite (200–500 °C) and for micro-sized particles (500 and 600 °C)<sup>33</sup> and cation doping has been found to be a useful tool to enhance the transition temperature. Doping of amorphous Fe<sub>2</sub>O<sub>3</sub> with 8.5% Mn<sup>3+</sup> led to  $\gamma$ -Fe<sub>2</sub>O<sub>3</sub> nanoparticles after heating for 3 hours at 500 °C<sup>34</sup> and Zn<sup>2+</sup> doping enhances the phase transformation temperature by *circa* 100 °C.<sup>35</sup> DSC studies under air of Zn<sub>x</sub>Fe<sub>3-x</sub>O<sub>4</sub> ( $x = 0, 0.2, 0.4$ , and  $0.6$ ) solid solution showed that the  $\gamma$ -Fe<sub>2</sub>O<sub>3</sub> to  $\alpha$ -Fe<sub>2</sub>O<sub>3</sub> phase transition temperature increases with increase in zinc content.<sup>36</sup> A study on Fe<sub>3-x</sub>Co<sub>x</sub>O<sub>4</sub> solid solutions showed that for  $x = 0.1$  the temperature of the  $\gamma$ -Fe<sub>2</sub>O<sub>3</sub> to  $\alpha$ -Fe<sub>2</sub>O<sub>3</sub> transition was increased by about 100 °C.<sup>37</sup>  $\gamma$ -Fe<sub>2</sub>O<sub>3</sub> nanoparticles doped with La<sup>3+</sup> showed no sign of phase transition to  $\alpha$ -Fe<sub>2</sub>O<sub>3</sub> after 8 hours at 400 °C.<sup>38</sup>

Here, we show that the  $\gamma$ -Fe<sub>2</sub>O<sub>3</sub> to  $\alpha$ -Fe<sub>2</sub>O<sub>3</sub> transition temperature is enhanced up to 550 °C as a consequence of the reaction of  $\gamma$ -Fe<sub>2</sub>O<sub>3</sub> nanoparticles with ammonia. PXRD data show no changes in the patterns indicating no formation of nitrides, but it is likely that a thin layer of oxide-nitride is formed on the surface of the  $\gamma$ -Fe<sub>2</sub>O<sub>3</sub> nanoparticles. It has been reported that the  $\alpha/\gamma$  structural transition occurs as the size of the particles increases; hence an O/N layer is likely to decompose in air as the temperature increases (TGA carried out in air), hence delaying the  $\alpha/\gamma$  structural transition. Whether the presence of primary amines on the surface of  $\gamma$ -Fe<sub>2</sub>O<sub>3</sub> nanoparticles has any influence on the  $\gamma$ -Fe<sub>2</sub>O<sub>3</sub> to  $\alpha$ -Fe<sub>2</sub>O<sub>3</sub> transition temperature is difficult to assess. Functionalisation of  $\gamma$ -Fe<sub>2</sub>O<sub>3</sub> nanoparticles with palmitic acid was reported to shift the  $\gamma$ -Fe<sub>2</sub>O<sub>3</sub> to  $\alpha$ -Fe<sub>2</sub>O<sub>3</sub> transition temperature up to 400 °C.<sup>39</sup> Two sets of  $\gamma$ -Fe<sub>2</sub>O<sub>3</sub> nanoparticles were functionalised with PMMA (poly-methyl methacrylate) and with caprylate respectively and their  $\gamma$  versus  $\alpha$  phase stability compared.<sup>40</sup> The  $\gamma$ -Fe<sub>2</sub>O<sub>3</sub> to  $\alpha$ -Fe<sub>2</sub>O<sub>3</sub> transition occurred at 400 °C for the caprylate-capped  $\gamma$ -Fe<sub>2</sub>O<sub>3</sub> nanoparticles and at 500 °C for the  $\gamma$ -Fe<sub>2</sub>O<sub>3</sub>/PMMA composite



$\gamma$ -Fe<sub>2</sub>O<sub>3</sub>. It was argued that the outer molecular layer creates a barrier, which slows down the aggregation of the nanoparticles and consequent structural transition. However, in our case the coating of the nanoparticles alone may not be very effective in hindering particle aggregation as -NH<sub>2</sub> groups provide an outer layer of comparable thickness to the -OH layers.

## Conclusion

In summary, we prepared  $\gamma$ -Fe<sub>2</sub>O<sub>3</sub> nanoparticles and reacted them with NH<sub>3</sub> (g) at 200 °C for 1 and 2 hours. We obtained directly amine-functionalised  $\gamma$ -Fe<sub>2</sub>O<sub>3</sub> nanoparticles, *i.e.*  $\gamma$ -Fe<sub>2</sub>O<sub>3</sub> nanoparticles with NH<sub>2</sub> groups substituting -OH surface groups. Normally, a silica shell is needed to prepare amine-functionalised  $\gamma$ -Fe<sub>2</sub>O<sub>3</sub> nanoparticles; however, this additional layer contributes to increasing the size of the nanoparticles, a disadvantage for medical applications. The amine-functionalised nanoparticles did not show any sizeable increase in their diameter, were re-dispersed in water to form stable ferrofluids and showed, therefore, suitability for reactions with application-controlling molecules. TGA coupled with heat flow measurements showed that the presence of the amine layer and, probably, of an oxide-nitride surface layer also enhances the  $\gamma$ -Fe<sub>2</sub>O<sub>3</sub> to  $\alpha$ -Fe<sub>2</sub>O<sub>3</sub> transition temperature up to 550 °C, comparable to previously reported cation modifications.

## Notes and references

- 1 R. Massart, *IEEE Trans. Magn.*, 1981, **17**(2), 1247.
- 2 J.-C. Bacri, R. Perzynski, D. Salin, V. Cabuil and R. Massart, *J. Magn. Magn. Mater.*, 1986, **62**(1), 36.
- 3 K. Raj, B. Moskowitz and R. Casciari, *J. Magn. Magn. Mater.*, 1995, **149**(1–2), 174.
- 4 I. Sharifi, H. Shokrollahi and S. Amiri, *J. Magn. Magn. Mater.*, 2012, **324**(6), 903.
- 5 R. Banerjee, Y. Katsenovich, L. Lagos, M. McIntosh, X. Zhang and C.-Z. Li, *Curr. Med. Chem.*, 2010, **17**(27), 3120.
- 6 E. Amstad, M. Textor and E. Reimhult, *Nanoscale*, 2011, **3**, 2819.
- 7 T. Georgelin, V. Maurice, B. Malezieux, J.-M. Siaugue and V. Cabuil, *J. Nanopart. Res.*, 2010, **12**(2), 675.
- 8 J. E. Jorgensen, L. Mosegaard, L. E. Thomsen, T. R. Jensen and J. C. Hanson, *J. Solid State Chem.*, 2007, **180**, 180.
- 9 C. Greaves, *J. Solid State Chem.*, 1983, **49**, 325.
- 10 T. J. Bastow, A. Trinchì, M. R. Hill, R. Harris and T. H. Muster, *J. Magn. Magn. Mater.*, 2009, **321**(17), 2677.
- 11 R. M. Cornel and U. Schwertmann, *The Iron Oxides. Structure, Properties, Reactions and Uses*, 2003.
- 12 D.-D. Lee and D.-H. Choi, *Sens. Actuators, B*, 1990, **1**, 231.
- 13 N. Fauconnier, A. Bée, J. Roger and J. N. Pons, *J. Mol. Liq.*, 1999, **83**(1–3), 233.
- 14 W. Kim, C.-Y. Suh, S.-W. Cho, K.-M. Roh, H. Kwon, K. Song and I.-J. Shon, *Talanta*, 2012, **94**, 348.
- 15 O. S. Wolfbeis, M. Hof, R. Hutterer and V. Fidler, *Fluorescence Spectroscopy in Biology*, Springer, Berlin, 2005.
- 16 R. Kellener, F. Lottspeich and H. E. Meer, *Microcharacterization of Proteins*, 2nd edn, 1999.
- 17 A. C. Larson and R. B. Von Dreele, General Structure Analysis System (GSAS), *Los Alamos National Laboratory Report LAUR 86-748*, 2004.
- 18 B. H. Toby, EXPGUI, *J. Appl. Crystallogr.*, 2001, **34**, 210.
- 19 V. Petkov, P. D. Cozzoli, R. Buonsanti, R. Cingolani and Y. Ren, *J. Am. Chem. Soc.*, 2009, **131**, 14264–14266.
- 20 X. L. Wu, W. Zhong, N. J. Tang, H. Y. Jiang, W. Liu and Y. W. Du, *J. Alloys Compd.*, 2004, **385**, 294.
- 21 S. Kurian and N. S. Gajbhiye, *J. Nanopart. Res.*, 2010, **12**, 1197.
- 22 S. Kurian and N. S. Gajbhiye, *Chem. Phys. Lett.*, 2010, **493**, 299.
- 23 W. Arabczyk, J. Zamlynny and D. Moszynski, *Pol. J. Chem. Technol.*, 2010, **12**, 38.
- 24 F. Tessier, *Solid State Sci.*, 2000, **2**, 457.
- 25 S. Kikkawa, K. Kubota and T. Takeda, *J. Alloys Compd.*, 2008, **449**, 7.
- 26 N. N. Greenwood and T. C. Gibb, *Mössbauer Spectroscopy*, 1971, ch. 10, pp. 240–258.
- 27 Y. R. Uhm, W. W. Kim and C. K. Rhee, *Phys. Status Solidi A*, 2004, **201**, 1934.
- 28 E. Darezereshki, *Mater. Lett.*, 2011, **65**, 642.
- 29 L. Machala, J. Tuek and R. Zbořil, *Chem. Mater.*, 2011, **23**, 3255.
- 30 X. Ye, D. Lin, Z. Jiao and L. Zhang, *J. Phys. D: Appl. Phys.*, 1998, **31**, 2739.
- 31 T. Belina, N. Millot, N. Bovet and M. Gailhanou, *J. Solid State Chem.*, 2007, **180**, 2377.
- 32 G. Schimanke and M. Martin, *Solid State Ionics*, 2000, **136**, 1235.
- 33 G. Ennas, A. Mei, A. Musinu, G. Piccaluga, G. Pinna and S. Solinas, *J. Mater. Res.*, 1999, **14**(4), 1570.
- 34 J. Lai, K. V. P. M. Shafi, K. Loos, A. Ulman, Y. Lee, T. Vogt and C. Estournes, *J. Am. Chem. Soc.*, 2003, **125**, 11470.
- 35 S. Deka and P. A. Joy, *J. Mater. Chem.*, 2007, **17**, 453.
- 36 S. S. Pati and J. Philip, *J. Appl. Phys.*, 2013, **113**(4), 044314/1.
- 37 S. S. Pati, S. Gopinath, G. Panneerselvam, M. P. Antony and J. Philip, *J. Appl. Phys.*, 2012, **112**(5), 054320/1.
- 38 H. Wang, N. Hua, Y. Du and P. Yang, *Huaxue Yanjiu Yu Yingyong*, 2005, **17**(3), 369.
- 39 R. Zboril, A. Bakandritsos, M. Mashlan, V. Tzitzios, P. Dallas, C. Trapalis and D. Petridis, *Nanotechnology*, 2008, **19**, 095602.
- 40 T. Ninjbadgar, S. Yamamoto and M. Takano, *Solid State Sci.*, 2005, **7**, 33.

